ELSEVIER

Neurobiology of Aging 28 (2007) 91–98

NEUROBIOLOGY OF AGING

www.elsevier.com/locate/neuaging

The aging brain: Accumulation of DNA damage or neuron loss?

Bart P.F. Rutten [a,b,1], Christoph Schmitz [a,b,*,1], Oliver H.H. Gerlach [a], Hans M. Oyen [a], Emmily Bueno de Mesquita [a], Harry W.M. Steinbusch [a,b], Hubert Korr [a,b,c]

[a] *Department of Psychiatry and Neuropsychology, Division of Cellular Neuroscience, Maastricht University, Universiteitssingel 50, 6200 MD Maastricht, The Netherlands*

[b] *European Graduate School of Neuroscience, EURON, Maastricht, The Netherlands*

[c] *Department of Anatomy and Cell Biology, RWTH Aachen University, Wendlingweg 2, 52057 Aachen, Germany*

Received 25 May 2005; received in revised form 25 October 2005; accepted 27 October 2005
Available online 9 December 2005

Abstract

Age-related molecular and cellular alterations in the central nervous system are known to show selectivity for certain cell types and brain regions. Among them age-related accumulation of nuclear (n) DNA damage can lead to irreversible loss of genetic information content. In the present study on the aging mouse brain, we observed a substantial increase in the amount of nDNA single-strand breaks in hippocampal pyramidal and granule cells as well as in cerebellar granule cells but not in cerebellar Purkinje cells. The reverse pattern was found for age-related reductions in total numbers of neurons. Only the total number of cerebellar Purkinje cells was significantly reduced during aging whereas the total numbers of hippocampal pyramidal and granule cells as well as of cerebellar granule cells were not. This formerly unknown inverse relation between age-related accumulation of nDNA damage and age-related loss of neurons may reflect a fundamental process of aging in the central nervous system.

Keywords: Aging; Nuclear DNA damage; Cell loss; In situ nick translation; Stereology; Hippocampus; Cerebellum; Cell type specificity; Selective neurovulnerability

1. Introduction

Compelling evidence in the literature points to a central role of accumulation of nuclear (n) DNA damage in the aging process of postmitotic cells such as neurons in the central nervous system (CNS) [20,21]. However, the aging process does not affect the CNS uniformly [29]. Rather various brain regions and types of neurons differ substantially in the amount of nDNA damage accumulation during aging [36]. Specifically, more nDNA damage was found in the aging hippocampus than in the aging cerebellum [27]. Furthermore, we have recently shown for the mouse brain that hippocampal pyramidal and granule cells were affected by an age-related decline in the amount of spontaneous nDNA repair whereas cerebellar Purkinje cells were not [41,42]. Noticeably, other studies on rodents have indicated an age-related reduction in the number of cerebellar Purkinje cells [43,47] whereas no alterations in the number of hippocampal pyramidal and granule cells as well as in the number of cerebellar granule cells were found during aging [32,43]. In this regard it is noteworthy to consider that at least hippocampal pyramidal cells as well as cerebellar granule and Purkinje cells are not replenished with age by neuronal progenitor cells [1,4,44]. Thus, hippocampal pyramidal cells, cerebellar granule cells and cerebellar Purkinje cells which might be lost during aging cannot be replaced by new cells. Based on these findings we have hypothesized [36] that neurons in the mammalian CNS show either an age-related increase in the amount of accumulated nDNA damage, connected with age-related decline in the ability to properly repair nDNA damage, or an age-related reduction in number. The aim of the present study was to test this hypothesis for the aging mouse brain. For this aim,

* Corresponding author. Tel.: +31 43 388 4108; fax: +31 43 367 1096.
E-mail address: c.schmitz@np.unimaas.nl (C. Schmitz).
[1] These authors contributed equally to this work.

0197-4580/$ – see front matter © 2005 Elsevier Inc. All rights reserved.
doi:10.1016/j.neurobiolaging.2005.10.019

both the relative amount of nDNA single-strand breaks and the total numbers of cells were measured for hippocampal pyramidal and granule cells as well as for cerebellar granule and Purkinje cells in adult and aged animals taken from the same cohort of mice aged under controlled conditions.

2. Methods

2.1. Animals

A cohort of $n = 80$ male Han/NMRI mice was bred and housed under specified pathogen free conditions at the Institut für Versuchstierkunde, RWTH Aachen University, Aachen, Germany (four animals per cage, air-conditioned rooms, 20 °C, 60% humidity, 12:12 h light:dark cycle with artificial lights on at 6:00 a.m., ad libitum access to water and Altromin standard diet [Altromin, Lage, Germany]). All experiments and investigations were performed in accordance with German animal protection law. Of these mice, $n = 56$ were allowed to die spontaneously (control group; mean age 25.7 ± 3.29 months [mean ± standard deviation; S.D.]; median [50%] survival 26.1 months; maximum survival 30.3 months; data provided as requested for experimental aging research in [30]) (Fig. 1). The remaining mice were sacrificed at 11.3 ± 0.8 months of age ($n = 12$; "adult mice"; 100% survival of the control group) as well as at 27.8 ± 0.3 months of age ($n = 12$; "aged mice"; 28% survival of the control group). Six adult and six aged mice were analyzed with high-precision design-based stereology [39,40,46] for volumes of brain regions and region-specific total numbers of neurons; the remaining six adult and six aged mice were investigated with in situ nick translation in combination with quantitative autoradiography [21] in a cell type specific manner in situ for the relative amount of nDNA single-strand breaks. Due to differences in requirements for optimum tissue fixation stereologic analyses and investigations of nDNA single-strand breaks could not be done on the same animals.

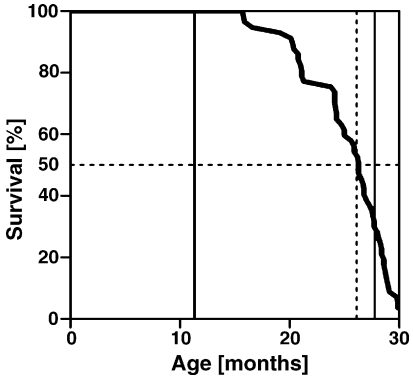

Fig. 1. Survival curve of the mice who died spontaneously (control group; $n = 56$). The dashed vertical line indicates 50% survival of the cohort (26.1 months). The solid vertical lines indicate the time points at which adult mice (mean age 11.3 months) and aged mice (mean age 27.8 months) were sacrificed for analysis.

To prevent bias in the analyses, it was guaranteed that each animal selected for analysis had the same chance to be investigated either with stereology or with ISNT. Furthermore, the mice did not show obvious alterations in the patterns of sleep and activity during aging, which could affect both nDNA damage and nDNA repair [14].

2.2. Analysis of volumes of brain regions and total numbers of neurons

$N = 6$ adult mice (mean age = 12.0 ± 0 months; mean ± S.D.) and $n = 6$ aged mice (mean age = 27.8 ± 0.3 months) were anesthetized with chloral hydrate (10% aqueous solution, 0.005 ml/g body weight, intraperitoneally) and were sacrificed by intracardial perfusion fixation with formalin solutions as previously described [37]. After opening the skulls, the heads of the animals were postfixed in formalin solution for 24 h at 4 °C. Afterwards the brains were removed, hemisected exactly in the midsagittal line, and further fixed in formalin solution for 10 days at 4 °C. Both brain halves were cryoprotected in sucrose solution (10%, 20% and finally 30% sucrose in 0.1 M Tris–HCl buffer, 2 × 12 h per solution; 4 °C), embedded in Tissue-Tek® (Sakura Finetek) and quickly frozen. Both brain halves were stored at −70 °C. The right brain halves were entirely cut on a cryostat (Type HM 500 OMV, Microm, Walldorf, Germany) to serial, 30 μm thick frontal sections. Every third section was selected, mounted on a glass slide, dried, defatted with Triton X-100 and stained with cresyl violet as previously described [37]. Slides were coverslipped using DePeX (Serva, Heidelberg, Germany). The left brain halves were not used in the present study and were stored for future experiments.

Stereologic measurements were performed with a stereology workstation, consisting of a modified light microscope (Olympus BX50; Olympus, Tokyo, Japan), Olympus UplanApo objectives (10×, NA = 0.40; 40×, oil, NA = 1.0; 100×, oil, NA = 1.35), motorized specimen stage for automatic sampling (Ludl, Hawthorne, NY, USA), electronic microcator (Ludl), CCD color video camera (Hitachi, Tokjo, Japan), PC (CoWoTec, Magdeburg, Germany) with framegrabber board, and stereology software (StereoInvestigator, MicroBrightField, Williston, VT, USA). After exactly tracing the boundaries of hippocampal pyramidal cell layer (CA1-3), hippocampal granule cell layer and hippocampal white matter as well as of cerebellar molecular layer, cerebellar granule cell layer and cerebellar white matter (using the 10× objective) on video images displayed on the monitor, the volumes of the chosen brain regions were calculated with Cavalieri's principle [8,40] considering the average actual section thickness after histological processing. The latter was measured with the electronic microcator. Total numbers of hippocampal pyramidal cells (CA1-3) and hippocampal granule cells as well as of cerebellar granule and Purkinje cells were evaluated with the optical fractionator [39,40,46]. All neurons whose nucleus top came into focus within

Table 1
Details of the stereologic analyses to estimate total numbers of neurons

Type of neuron	Obj.	B (μm^2)	H (μm^2)	D (μm)	t (μm)	Σ OD	Σ Q^-	$CE_{pred}(n)$
Hi-PC	100×	900	4	141	8.7	313	913	0.034
Hi-GC	100×	625	4	100	8.5	203	919	0.034
Ce-GC	100×	64	5	250	10.2	446	1.555	0.026
Ce-PC	40×	3600	5	220	10.9	261	507	0.045

Hi-PC, hippocampal pyramidal cells (CA1-3); Hi-GC, hippocampal granule cells; Ce-GC; cerebellar granule cells; Ce-PC, cerebellar Purkinje cells. Obj., objective used; B and H, base and height of the unbiased virtual counting spaces; D, distance between the unbiased virtual counting spaces in mutually orthogonal directions x and y; t, measured actual average section thickness after histological processing; Σ OD, average sum of unbiased virtual counting spaces used; Σ Q^-, average number of counted neurons; $CE_{pred}(n)$, average predicted coefficient of error of the estimated total numbers of neurons using the prediction method described in [38,39].

unbiased virtual counting spaces distributed in a systematic-random fashion throughout the delineated regions were counted. Estimated total numbers of neurons were calculated from the numbers of counted neurons and the corresponding sampling probability. Details of the counting procedure are summarized in Table 1. All measurements were performed by the same person blinded for the age of the mice.

2.3. Analysis of the relative amount of n DNA single-strand breaks

$N = 6$ adult mice (mean age = 10.7 ± 0.5 months) and $n = 6$ aged mice (mean age = 27.8 ± 0.3 months) were sacrificed by cervical dislocation. The brains were immediately dissected out and hemisected exactly in the midsagittal line. Right and left brain halves were embedded in Tissue-Tek® (Sakura Finetek Europe, Zoeterwoude, The Netherlands) and quickly frozen using a solution of aceton/dry ice at −68 °C. The right brain halves were cut into 10 μm thick sagittal sections including the hippocampus and the cerebellum on a cryostat (type HM 500 OM; Microm, Walldorf, Germany). The sections were mounted on glass slides (SuperFrost Plus, Menzel, Braunschweig, Germany) and stored at −70 °C until further processing. The left brain halves were not used in the present study and were stored for future experiments.

The relative amount of nDNA single-strand breaks was investigated by means of in situ nick translation (ISNT), carried out using a slight modification of the protocol given by Maehara et al. [26] as described in Korr et al. [21]. Briefly, sections were incubated for 60 min at 37 °C with a reaction solution containing 50 mM Tris–HCl-buffer (pH 7.5), 5 mM $MgCl_2$, 10 mM 2-mercaptoethanol, 200 U/ml of *E. coli* DNA polymerase I (endonuclease-free, Boehringer, Mannheim, Germany), 10 μmol/ml each of dATP, dGTP, dCTP and dTTP (Boehringer) and 15 μl [^{3}H]dTTP/ml (1.03 MBq/ml; American Radiolabeled Chemicals Inc., St. Louis, MO). Incubation was carried out using special in situ chambers consisting of small frames made of silicon (height = 1 mm; comparable to customary adapters for in situ PCR) and coverslips placed onto the slides. The reaction was terminated by washing the slides with 50 mM Tris–HCl buffer (pH 7.5). Afterwards the sections were Feulgen stained, dipped into diluted Ilford K2 emulsion (3:2 with distilled water) at 42 °C, exposed for 5 days at 4 °C and developed in Amidol (4 min, 18 °C). After poststaining with hematoxylin the autoradiographs were covered with a coverslip using Entellan® (Merck, Darmstadt, Germany).

Evaluation of the autoradiographs was carried out with a light microscope (Olympus BH-2 equipped with a 100× oil Olympus UplanFl objective, NA = 1.30). For each animal, two randomly selected, non-adjacent coded autoradiographs showing the hippocampus as well as two autoradiographs showing the cerebellum were selected. On each section 50 randomly selected cell profiles of each of the following types of neurons were investigated regarding the number of autoradiographic silver grains over the nucleus: hippocampal pyramidal cells (area CA1-3), hippocampal granule cells (dentate gyrus), cerebellar granule cells, and cerebellar Purkinje cells. Counting of silver grains of all types of neurons was performed by the same person blinded for the age of the mice. Background was corrected by investigating autoradiographs which were prepared in an identical manner as described above except for the application of DNA polymerase I [21]. Furthermore, data were corrected for nuclear size, allowing direct comparisons between different cell types [21]. Again all measurements were performed by the same person blinded for the age of the mice.

2.4. Statistical analysis

For each group of mice, mean and standard error of the mean were calculated for the estimated volumes of the investigated brain regions, the estimated total numbers of neurons, and the cell-type specific autoradiographic silver grain numbers per nucleus (corrected for background and nuclear size). Comparisons between adult and aged animals were performed with two-tailed unpaired Student's t test. Statistical significance was established at $p < 0.05/4$ (i.e., 0.0125) considering Bonferroni correction, since four different types of neurons were investigated simultaneously (hippocampal white matter, cerebellar molecular layer and cerebellar white matter were not considered here). Calculations were performed using GraphPad Prism (Version 4.00 for Windows, GraphPad Software, San Diego, CA).

Furthermore, for each animal and type of neuron, the frequency distribution of the 100 obtained (uncorrected)

numbers of autoradiographic silver grains was calculated, with bin width of one and the center of the first bin at zero. These frequency distributions were used to calculate age-specific, averaged frequency distributions of uncorrected numbers of autoradiographic silver grains for each type of neuron. For instance, the $n = 6$ adult mice showed the following frequencies of hippocampal pyramidal cells with a total of six autoradiographic silver grains over the nucleus: 14, 6, 16, 8, 10, 18. Accordingly, the average frequency of hippocampal pyramidal cells in the brains from the adult mice with a total of six autoradiographic silver grains over the nucleus was 12. These averaged frequency distributions of the adult mice were compared with the corresponding averaged frequency distributions of the aged mice using the Kolmogorov–Smirnov two sample test. Comparing averaged frequency distributions considered the fact that the 95% critical value ($\alpha = 0.05$) for the Kolmogorov–Smirnov two sample test depends on the number of data points (which was 200 when comparing two groups with 100 data points each). Statistical significance was established at $p < 0.0125$ considering Bonferroni correction, since four different types of neurons were investigated simultaneously. These calculations were performed using SPSS (Version 11.5.0 for Windows; SPSS, Chicago, IL).

3. Results

3.1. Volumes of brain regions

We found no differences between adult and aged mice in mean volumes of hippocampal pyramidal cell layer (CA1-3) ($p = 0.281$; Fig. 2A), hippocampal granule cell layer ($p = 0.529$; Fig. 2B) and cerebellar granule cell layer ($p = 0.630$; Fig. 2C) as well as of hippocampal white matter ($p = 0.453$; Fig. 2M), cerebellar molecular layer ($p = 0.740$; Fig. 2N) and cerebellar white matter ($p = 0.747$; Fig. 2O).

3.2. Total numbers of neurons

Adult and aged mice did not differ in mean total numbers of hippocampal pyramidal cells ($p = 0.539$; Fig. 2D), hippocampal granule cells ($p = 0.583$; Fig. 2E) and cerebellar granule cells ($p = 0.560$; Fig. 2F). In contrast, the mean total number of cerebellar Purkinje cells was significantly reduced in the aged mice compared with the adult ones (−25.2%, $p = 0.009$; Fig. 2G).

3.3. Relative amount of nDNA single-strand breaks

For hippocampal pyramidal and granule cells as well as for cerebellar granule cells – but not for cerebellar Purkinje cells – significantly different averaged frequency distributions of uncorrected numbers of autoradiographic silver grains were found when comparing adult with aged mice ($p < 0.001$ for hippocampal pyramidal and granule cells as well as for cerebellar granule cells, $p = 0.587$ for cerebellar Purkinje cells) (Fig. 3). The cumulated relative frequency distributions of uncorrected numbers of autoradiographic silver grains of hippocampal pyramidal and granule cells as well as of cerebellar granule cells from the aged mice were shifted to the right compared with the corresponding frequency distributions from

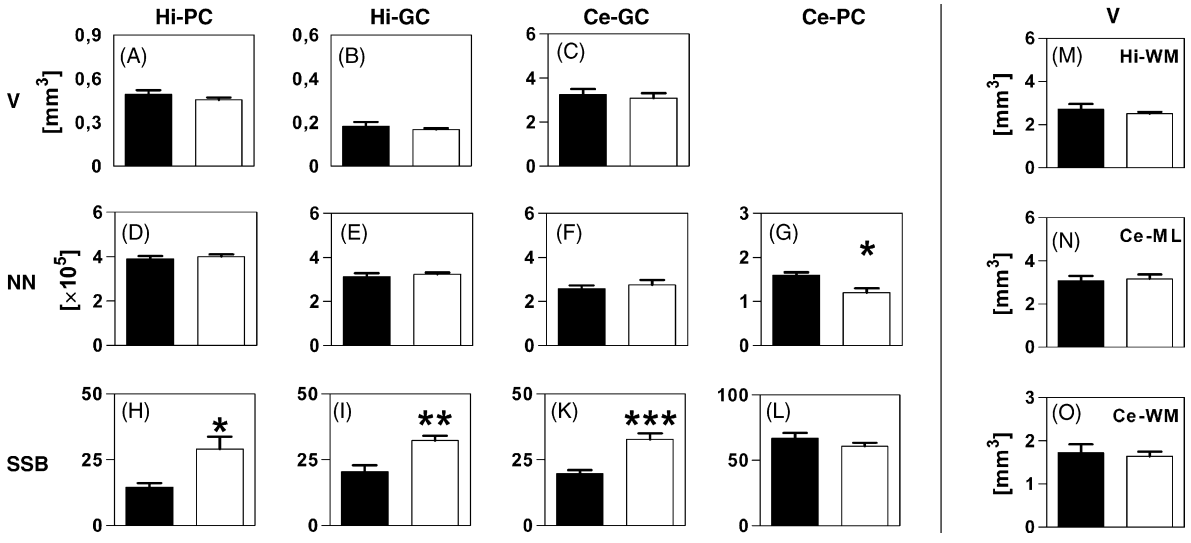

Fig. 2. Mean and standard error of the mean (S.E.M.) of volumes of hippocampal pyramidal cell layer [Hi-PC] (A), hippocampal granule cell layer [Hi-GC] (B), cerebellar granule cell layer [Ce-GC] (C), hippocampal white matter [Hi-WM] (M), cerebellar molecular layer [Ce-ML] (N) and cerebellar white matter [Ce-WM] (O), mean ± S.E.M. of total numbers of hippocampal pyramidal cells (D), hippocampal granule cells (E), cerebellar granule cells (F) and cerebellar Purkinje cells (G), and mean ± S.E.M. of mean autoradiographic silver grain counts corrected for background and nuclear size, representing the relative amount of nDNA single-strand breaks within hippocampal pyramidal cells (H), hippocampal granule cells (I), cerebellar granule cells (K) and cerebellar Purkinje cells (L). V, volume; NN, neuron number; SSB, nDNA single-strand breaks. Closed bars, adult animals; open bars, aged animals. $^{*}p < 0.0125$; $^{**}p < 0.005$; $^{***}p < 0.001$ (results from two-tailed unpaired Student's *t*-test).

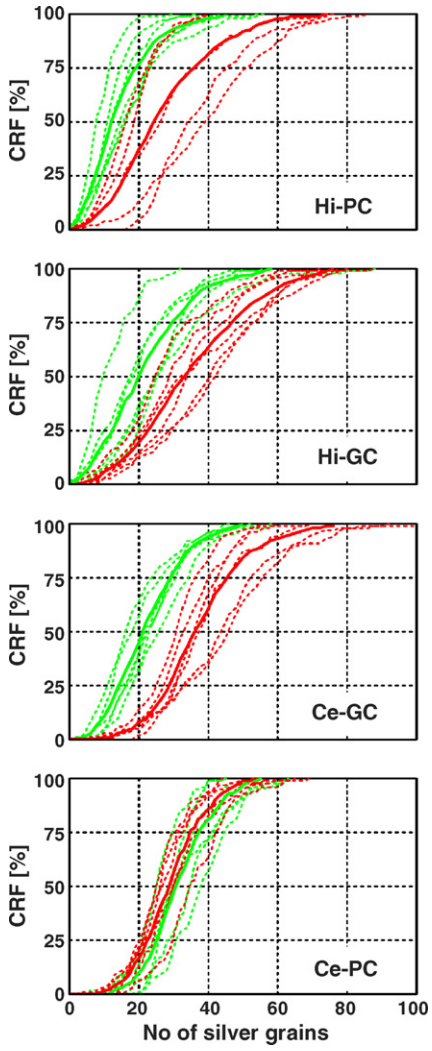

Fig. 3. Cumulated relative frequency (CRF) distributions of uncorrected numbers of autoradiographic silver grains from adult mice (green lines) and aged mice (red lines). Dotted lines, individual frequency distributions; solid lines, averaged frequency distributions. Hi-PC, hippocampal pyramidal cells; Hi-GC, hippocampal granule cells; Ce-GC, cerebellar granule cells; Ce-PC, cerebellar Purkinje cells.

the adult animals (Fig. 3). This indicated that the aged mice showed on average higher numbers of uncorrected autoradiographic silver grains per nucleus for hippocampal pyramidal and granule cells as well as for cerebellar granule cells, but not for cerebellar Purkinje cells.

Analysis of autoradiographic silver grains corrected for background and nuclear size resulted in the same finding. The mean corrected number of autoradiographic silver grains of hippocampal pyramidal and granule cells as well as of cerebellar granule cells was significantly higher in the aged mice than in the adult ones (+97.6% for hippocampal pyramidal cells in area CA1-3, $p = 0.012$; +57.4% for hippocampal granule cells, $p = 0.004$; and +65.3% for cerebellar granule cells, $p < 0.001$; Fig. 2H–K). Cerebellar Purkinje cells showed the highest mean corrected number of autoradiographic silver grains of all investigated types of neurons but did not show differences in mean numbers between aged and adult mice ($p = 0.226$; Fig. 2L).

In summary, the autoradiographic analysis with in situ nick translation demonstrated that cerebellar Purkinje cells had the highest relative amount of nDNA single-strand breaks of all investigated types of neurons. Age-related accumulation of nDNA single-strand breaks was observed for hippocampal pyramidal and granule cells as well as for cerebellar granule cells, but not for cerebellar Purkinje cells.

4. Discussion

The results of the present study are the first description of cell-type-specific alterations in the relative amount of nDNA single-strand breaks in situ in the mouse brain during aging, and extend earlier reports on region-specific accumulation of nDNA damage in the aging rodent brain [27] in a cell type specific manner. Based on the selection of aged mice at 28% survival of the control group, our results were neither biased by the "survival-of-the-fittest" effect (which can be observed at approximatly 40% survival of a cohort; see, e.g., [41]) nor by the "oldest-of-the-old" effect (which can be observed at approximatly 10% survival of a cohort; see, e.g., [17]). We investigated the relative amount of nDNA single-strand breaks as a measure of nDNA damage since this kind of nDNA damage is the only one which can be analyzed quantitatively in a cell-type specific manner in situ (with ISNT) [21,26]. Furthermore, nDNA single-strand breaks are the most common endogenous lesions arising in cells (thousands per cell per day), and are the most common lesions induced by exogenous genotoxins such as ionizing radiation and alkylating agents [3,5–7]. Direct nDNA single-strand breaks are characterized by the disintegration of damaged sugars and arise primarily from attack by free radicals such as reactive oxygen species. In contrast, indirect nDNA single-strand breaks are characterized by enzymatic cleavage of the phosphodiester backbone and are mainly normal intermediates of DNA base excision repair. Nuclear DNA single-strand breaks are probably not permanent breaks but are repaired by a process called single-strand break repair. The same group of proteins appear to repair both direct and indirect nDNA single-strand breaks [3,5–7]. Permanent nDNA damage is invisible to ISNT; neither ISNT can be used to measure mtDNA single-strand breaks in situ. However, a rise in the level of nDNA single-strand breaks can be the result of a shift in the balance between nDNA damage and nDNA repair, which has a very high fidelity. Thus, a higher level of nDNA single-strand breaks (and, thus, a higher signal in ISNT autoradiographs) can be interpreted as a higher steady state level of damaged nDNA in the investigated tissue.

Conflicting reports exist in the literature about age-related alterations in volumes of hippocampal and cerebellar gray and white matter. Our findings of no age-related alterations in any of the investigated hippocampal and cerebellar subregions in Han/NMRI mice are in line with data from Rapp et al.

[33] who found a decrease only in the volume of the middle portions of the dentate gyrus molecular layer, but not of several other hippocampal subregions, in aging Long-Evans rats. In line with these results, Keuker et al. [19] found no alterations in the volumes of subiculum and several hippocampal subregions (hilus, molecular layer and granule cell layer of the dentate gyrus, as well as areas CA1, CA2, CA3) in aging tree shrews. On the other hand, Dlugos and Pentney [13] reported an age-related decrease in the volume of the cerebellar molecular layer of male Fischer 344 rats. This discrepancy might be due to several reasons since *post mortem* analyses of volumes of brain regions on sections can be considerably affected by histological processing, which can affect gray and white matter differently [22]. This problem does not occur in estimates of total numbers of neurons performed with design-based stereology [40,46]. Accordingly, the results of our investigations on total numbers of hippocampal and cerebellar neurons with the optical fractionator are in line with various reports on cell type specific neuron loss in the rodent brain during aging (for details see ref. [36]).

Recently our group showed an age-related decline in the rate of spontaneous nDNA repair in hippocampal pyramidal and granule cells but not in cerebellar Purkinje cells (data of cerebellar granule cells were not unequivocal) by using quantitative autoradiography after injection of tritiated thymidine on the same animal model (i.e., same mouse strain, identical housing conditions at the same animal facility, almost identical survival curve) [41,42]. Together with these earlier findings, the results of the present study point to the existence of the following, so far unknown correlation between nDNA damage, nDNA repair and neuron loss in the aging mammalian brain: certain types of neurons (such as hippocampal pyramidal and granule cells as well as cerebellar granule cells) suffer from an age-related accumulation of nDNA damage, but these types of neurons are not reduced in number during aging. Other types of neurons (such as cerebellar Purkinje cells) are reduced in number during aging, but the remaining cells show no age-related accumulation of nDNA damage.

It is tempting to speculate whether this correlation between nDNA damage, nDNA repair and neuron loss in the aging mammalian brain reflects a causal link between these age-related alterations. One possible explanation could be that a certain threshold for nDNA damage exists, and cells in which this threshold is exceeded are eliminated. This explanation is in line with our observation that at 12 months of age, the relative amount of nDNA single-strand breaks in cerebellar Purkinje cells was approximately three-fold compared with the relative amount of nDNA single-strand breaks in hippocampal pyramidal and granule cells as well as in cerebellar granule cells. Most probably this high relative amount of nDNA single-strand breaks (reflecting a high steady state of nDNA damage) in cerebellar Purkinje cells is associated with the very high level of excitatory amino acid synaptic connections of cerebellar Purkinje cells as well as the exceptionally high metabolic demand of this cell type [45], making the cells selectively vulnerable under conditions such as acute hypoxia [9,45] or seizures [12]. On the other hand, our data point to the existence of (yet unknown) cell-type specific differences in responses to nDNA damage in the aging mammalian brain. This is due to the fact that hippocampal pyramidal and granule cells as well as cerebellar granule cells of the aged (i.e., 27.8 ± 0.3 months) mice showed relative amounts of nDNA single-strand breaks which were lower than the relative amount of nDNA single-strand breaks found in cerebellar Purkinje cells of the adult (i.e., 10.7 ± 0.5 months old) mice. However, age-related accumulation of nDNA damage plays a crucial role in impaired protein synthesis, increased production of free radicals and the formation of protein aggregations during aging, ultimately leading to severe cellular dysfunction [24,25]. In the human brain age-related DNA damage in the frontal cortex was reported to be associated with reduced expression of genes involved in synaptic plasticity, vesicular transport and mitochondrial function, followed by the induction of genes involved in stress response, antioxidant response and DNA repair [25]. There is no evidence in the literature that Purkinje cells in the cerebellum of mice specifically suffer from these impairments already at 11 months of age. It will thus be important to identify cell-type-specific differences in response mechanisms to nDNA damage in neurons in vivo, and alterations of these mechanisms during aging.

It has repeatedly been hypothesized that accumulation of nDNA damage (or, in a broader sense, the inability of neurons to appropriately handle nDNA damage) may serve as molecular "trigger" in the etiology of neurodegenerative diseases such as Alzheimer's disease (AD) [11,18,36], Parkinson's disease (PD) [34], Huntington's disease [35], amyotrophic lateral sclerosis [2] and spinocerebellar ataxia with axonal neuropathy-1 (SCAN1) [15]. On the other hand, these diseases show different selective neuronal vulnerabilities, indicating that other mechanisms than just the inability to appropriately handle nDNA damage must be involved in the corresponding etiologies. Indeed, research over the last decades has identified these mechanisms, such as the role of beta-amyloid in AD [16], alpha synuclein in PD [28] or huntingtin in HD [23]. However, the results of this research have not disproved the hypothesis of inappropriate handling of nDNA damage being involved in the etiology of these diseases. We have argued that cell-type specific differences in accumulation of nDNA damage during aging (as demonstrated in the present study for the mouse brain) might be involved in the selective neuronal vulnerability of AD [36,42]. In this regard a very recent study by Rademakers et al. [31] found evidence for linkage of AD with a candidate region at chromosome 7q36. A mutation analysis of coding exons of 29 candidate genes within this region identified one linked synonymous mutation in exon 10 (affecting codon 626) of the PAX transactivation domain interacting protein (PAXIP1) gene [31]. It has been indicated that PAXIP1 might be involved in nDNA repair [10], suggesting that the results of Rademakers et al. [31] might indicate a role of accumulation of nDNA damage due to improper nDNA repair in the

etiology of AD [11,18,36]. In this regard the aging mouse brain might be an attractive animal model to address potential links between the cause of cell-type specific differences in age-related accumulation of nDNA damage in neurons and the selective neuronal vulnerability in AD.

Acknowledgments

This work was supported by the Dutch Brain Foundation (Hersenstichting Nederland) and the International Alzheimer's Research Foundation (ISAO; the Netherlands).

References

[1] Abrous DN, Koehl M, Le Moal M. Adult neurogenesis: from precursors to network and physiology. Physiol Rev 2005;85:523–69.
[2] Armon C. Acquired nucleic acid changes may trigger sporadic amyotrophic lateral sclerosis. Muscle Nerve 2005;32:373–7.
[3] Bohr VA. Repair of oxidative DNA damage in nuclear and mitochondrial DNA, and some changes with aging in mammalian cells. Free Radic Biol Med 2002;32:804–12.
[4] Brazel CY, Rao MS. Aging and neuronal replacement. Ageing Res Rev 2004;3:465–83.
[5] Caldecott KW. Mammalian DNA single-strand break repair: an X-ra(y)ted affair. Bioessays 2001;23:447–55.
[6] Caldecott KW. XRCC1 and DNA strand break repair. DNA Repair 2003;2:955–69.
[7] Caldecott KW. DNA single-strand breaks and neurodegeneration. DNA Repair 2004;3:875–82.
[8] Cavalieri B. Geometria indivisibilibus continuorum. Typis Clementis Ferronij, Bononiae, 1635 (reprinted 1966 as Geometria Degli Indivisibili. Unione Tipografico-Editrice Torinese, Torino).
[9] Cervos-Navarro J, Diemer NH. Selective vulnerability in brain hypoxia. Crit Rev Neurobiol 1991;6:149–82.
[10] Cho EA, Prindle MJ, Dressler GR. BRCT domain-containing protein PTIP is essential for progression through mitosis. Mol Cell Biol 2003;23:1666–73.
[11] Cotman CW, Su JH. Mechanisms of neuronal death in Alzheimer's disease. Brain Pathol 1996;6:493–506.
[12] Dam M, Bolwig T, Hertz M, Bajorec J, Lomax P, Dam AM. Does seizure activity produce Purkinje cell loss? Epilepsia 1984;25:747–51.
[13] Dlugos CA, Pentney RJ. Morphometric analyses of Purkinje and granule cells in aging F344 rats. Neurobiol Aging 1994;15:435–40.
[14] Duffy PH, Feuers RJ. Biomarkers of aging: changes in circadian rhythms related to the modulation of metabolic output. Biomed Environ Sci 1991;4:182–91.
[15] El-Khamisy SF, Saifi GM, Weinfeld M, Johansson F, Helleday T, Lupski JR, et al. Defective DNA single-strand break repair in spinocerebellar ataxia with axonal neuropathy-1. Nature 2005;434:108–13.
[16] Gouras GK, Almeida CG, Takahashi RH, Intraneuronal. A beta accumulation and origin of plaques in Alzheimer's disease. Neurobiol Aging 2005;26:1235–44.
[17] Gower AJ, Lamberty Y. The aged mouse as a model of cognitive decline with special emphasis on studies in NMRI mice. Behav Brain Res 1993;57:163–73.
[18] Itzhaki RF. Possible factors in the etiology of Alzheimer's disease. Mol Neurobiol 1994;9:1–13.
[19] Keuker JI, de Biurrun G, Luiten PG, Fuchs E. Preservation of hippocampal neuron numbers and hippocampal subfield volumes in behaviorally characterized aged tree shrews. J Comp Neurol 2004;468:509–17.
[20] Kirkwood TB, Austas SN. Why do we age? Nature 2000;408:223–38.
[21] Korr H, Rohde HT, Benders J, Dafotakis M, Grolms N, Schmitz C. Neuron loss during early adulthood following prenatal low-dose X-irradiation in the mouse brain. Int J Radiat Biol 2001;77:567–80.
[22] Kretschmann HJ, Tafesse U, Herrmann A. Different volume changes of cerebral cortex and white matter during histological preparation. Microsc Acta 1982;86:13–24.
[23] Landles C, Bates GP. Huntingtin and the molecular pathogenesis of Huntington's disease. Fourth in molecular medicine review series. EMBO Rep 2004;5:958–63.
[24] Lieber MR, Karanjawala ZE. Ageing, repetitive genomes and DNA damage. Nat Rev Mol Cell Biol 2004;5:69–75.
[25] Lu T, Pan Y, Kao SY, Li C, Kohane I, Chan J, et al. Gene regulation and DNA damage in the ageing human brain. Nature 2004;429:883–91.
[26] Maehara Y, Anai H, Kusumoto T, Sakaguchi Y, Sugimachi K. Nick translation detection in situ of cellular DNA strand break induced by radiation. Am J Pathol 1989;134:7–10.
[27] Mandavilli BS, Rao KS. Neurons in the cerebral cortex are most susceptible to DNA-damage in aging rat brain. Biochem Mol Biol Int 1996;40:507–14.
[28] Moore DJ, West AB, Dawson VL, Dawson TM. Molecular pathophysiology of Parkinson's disease. Annu Rev Neurosci 2005;28:57–87.
[29] Morrison JH, Hof PR. Selective vulnerability of corticocortical and hippocampal circuits in aging and Alzheimer's disease. Prog Brain Res 2002;136:467–86.
[30] Mos J, Hollander CF. Analysis of survival data on aging rat cohorts: pitfalls and some practical considerations. Mech Ageing Dev 1987;38:89–105.
[31] Rademakers R, Cruts M, Sleegers K, Dermaut B, Theuns J, Aulchenko Y, et al. Linkage and association studies identify a novel locus for Alzheimer disease at 7q36 in a dutch population-based sample. Am J Hum Genet 2005;77:643–52.
[32] Rapp PR, Gallagher M. Preserved neuron number in the hippocampus of aged rats with spatial learning deficits. Proc Natl Acad Sci USA 1996;93:9926–30.
[33] Rapp PR, Stack EC, Gallagher M. Morphometric studies of the aged hippocampus. I. Volumetric analysis in behaviorally characterized rats. J Comp Neurol 1999;403:459–70.
[34] Robbins JH. Parkinson's disease, twins, and the DNA-damage hypothesis. Ann Neurol 1987;21:412.
[35] Robison SH, Bradley WG. DNA damage and chronic neuronal degenerations. J Neurol Sci 1984;64:11–20.
[36] Rutten BP, Korr H, Steinbusch HW, Schmitz C. The aging brain: less neurons could be better. Mech Ageing Dev 2003;124:349–55.
[37] Rutten BP, Wirths O, Van de Berg WD, Lichtenthaler SF, Vehoff J, Steinbusch HW, et al. No alterations of hippocampal neuronal number and synaptic bouton number in a transgenic mouse model expressing the beta-cleaved C-terminal APP fragment. Neurobiol Dis 2003;12:110–20.
[38] Schmitz C. Variation of fractionator estimates and its prediction. Anat Embryol 1998;198:371–97.
[39] Schmitz C, Hof PR. Recommendations for straightforward and rigorous methods of counting neurons based on a computer simulation approach. J Chem Neuroanat 2000;20:93–114.
[40] Schmitz C, Hof PR. Design-based stereology in neuroscience. Neuroscience 2005;130:813–31.
[41] Schmitz C, Axmacher B, Zunker U, Korr H. Age-related changes of DNA repair and mitochondrial DNA synthesis in the mouse brain. Acta Neuropathol 1999;97:71–81.
[42] Schmitz C, Materne S, Korr H. Cell-type-specific differences in age-related changes of dna repair in the mouse brain—molecular basis for a new approach to understand the selective neuronal vulnerability in Alzheimer's disease. J Alzheimers Dis 1999;1:387–407.
[43] Sturrock RR. Changes in neuron number in the cerebellar cortex of the ageing mouse. J Hirnforsch 1989;30:499–503.

[44] Turlejski K, Djavadian R. Life-long stability of neurons: a century of research on neurogenesis, neuronal death and neuron quantification in adult CNS. Prog Brain Res 2002;136:39–65.
[45] Welsh JP, Yuen G, Placantonakis DG, Vu TQ, Haiss F, O'Hearn E, et al. Why do Purkinje cells die so easily after global brain ischemia? Aldolase C, EAAT4, and the cerebellar contribution to posthypoxic myoclonus. Adv Neurol 2002;89:331–59.
[46] West MJ. New stereological methods for counting neurons. Neurobiol Aging 1993;14:275–85.
[47] Zanjani H, Lemaigre-Dubreuil Y, Tillakaratne NJ, Blokhin A, McMahon RP, Tobin AJ, et al. Cerebellar Purkinje cell loss in aging Hu-Bcl-2 transgenic mice. J Comp Neurol 2004;475: 481–92.